Fracture Toughness Characterization of a PC/ABS Blend Under Different Strain Rates By Various J-Integral Methods

MING-LUEN LU, KUO-CHAN CHIOU, *and* FENG-CHIH CHANG*

Institute of Applied Chemistry
National Chiao Tung University
Hsin-Chu, 30050 Taiwan, Republic of China

A published, nonconventional *J*-integral method, based on the hysteresis energy and the ASTM E813 methods, has been employed to test the fracture toughness of a polycarbonate (PC)/acrylonitrile-butadiene-styrene (ABS) blend. The critical *J* values (J_{Ic}) at crosshead speeds ranging from 0.5 to 20 mm/min obtained from the hysteresis energy method are ~10 to 20% higher than those obtained from the E813-81 method and ~50 to 70% lower than those obtained from the E813-87 method. However, the hysteresis energy method results in comparable J_{Ic} values with a modified ASTM E813-87 method when the 0.2 mm offset line is replaced with a 0.1 mm offset line. The critical displacements in terms of the onset of crack initiation, determined from the plots of hysteresis energy vs. displacement, hysteresis ratio vs. displacement, and the true crack growth length vs. displacement, are fairly close in value. This indicates the critical crack initiation and the corresponding J_{Ic} obtained from this hysteresis energy method indeed represent the actual physical event of the onset of crack initiation.

INTRODUCTION

By using the LEFM approach, the critical stress intensity factor K_{Ic}, defined as in ASTM E399, is used to characterize the fracture of brittle and rigid polymers (1). This approach employs the elastic analysis of the crack tip region. The size and geometry independent parameters, K_{Ic} and G_{Ic}, have been proven to represent the true material constants of many brittle polymers, provided that certain restrictive size criteria of the test specimen are satisfied to meet the requirements of plane-strain fracture. In these cases, the energy dissipation is limited only locally to the crack tip region, so that the behavior of the bulk is still elastic and the fracture can be derived from the energy change in an elastic analysis. However, linear elastic fracture mechanics is not suitable for most low-to-moderate and rubber-toughened polymers, because the problem of extensive plasticity at the crack tip has precluded the application of the criteria and the critical K_{Ic} and G_{Ic} are impractical to measure. Besides, a relatively larger specimen thickness required for LEFM to induce plane strain conditions is impractical experimentally. There are also difficulties in analysis of the stress field in the crack tip region. The preparation of thick specimens could cause molecular orientation and residual stresses (both can affect fracture toughness). These shortcomings from the LEFM approach induce the effort to seek other techniques that are suitable for polymers with extensive plastic yielding.

The earliest application of fracture mechanics to polymers was the work reported in 1953 by Rivlin and Thomas (2) on crack growth in crosslinked rubbers. These materials generally show a high degree of hysteresis in the intermediate vicinity of the crack tip, where large strains are experienced, and show nonlinear and elastically reversible behavior away from these regions. An approach to the problem of identifying a unique parameter to characterize the failure of the bodies with nonlinear and elastic behavior was developed principally by Rice (3, 4) to the crack growth in metals, which has been applied by several others, such as Turner (5), Chell (6), and Landes and Begley (7). Rice (3, 4) showed that a certain integral, now commonly called the *J*-integral, described the flow of energy into the crack tip region. The dominant term in the description of the stress and strain singularities at the crack tip can also be written in terms of *J*. He demonstrated that the value of *J* is independent of the integration path. However, it should be noted that the derivation of *J* is strictly valid only for linear and non-

* To whom correspondence should be addressed.

linear elastic materials where unloading occurs down the same path as the initial loading. For polymeric materials, the viscoelastic and plastic deformations make the unloading line follow a different path than the loading one. Nevertheless, in practice, the validity of J for materials that show this type of inelasticity or plasticity has been demonstrated experimentally by Landes and Begley (7) and supported by indirect analysis by Turner (5).

During the last decade, the J-integral methods have been applied successfully to numerous ductile polymeric materials using the multiple-specimen method developed by Begley and Landes (8, 9), or the single specimen method developed by Rice *et al.* (10). The crack growth of the single specimen method is measured by using an elastic unloading compliance technique (10). However, crack growth measured from a side-view may not be accurate, because the crack front may vary from the central region to the side sections. Therefore the J-values evaluated by this single-specimen method do not always agree with the values obtained from the standard multiple-specimen method. Westerlind *et al.* (11) used three different methods, namely the single-specimen, multiple-specimen, and Leibowitz nonlinear energy methods, to characterize the fracture toughness of linear board and report that the critical J values obtained by using this single-specimen method were greater than those obtained from the standard multiple-specimen method. Many authors have used the ASTM standards of E813-81 (12) and E813-87 (13) to characterize the fracture toughness of polymers (14–25).

Subsequently, numerous methodologies for J-integral testing and analysis have evolved. Yee and coworkers (26) employed a modified version of E813-81 to investigate the core-shell rubber modified polycarbonate. Chudnovsky and co-workers (27–30) developed the crack layer theory describing the crack propagation resistance in terms of material transformation preceding the crack tip (active zone) and applied it to several polymeric materials. Mai *et al.* (31–34) investigated the fracture toughness and fracture mechanisms of a PC/PBT/IM blend using an alternative to the J-integral method, the essential work analysis, which is experimentally simple and theoretically sound. Yuhara *et al.* (35) used a simplified method for evaluating the J-integral for paper sheet, which essentially employed the modification of the single-specimen technique. Joyce and Hackett (36) used the key curve method to measure the resistance curve of structural steels under impact conditions. Vu-Khanh (37) applied a different approach for determining impact fracture parameters of ductile polymers. Crouch and Huang (38) used the J-integral technique to characterize the toughness of rubber-toughened nylons under impact loading condition. A method of normalization was developed by Zhou, Landes, and Huang (39), to characterize the J-R curve fracture toughness of polymer materials, in which the direct measurement of the crack growth length is not required. This normalization method uses the plastic deformation character of material to determine indirectly the crack extension and the obtained results were then compared to those obtained from the multiple-specimen method of ASTM E813. Saze *et al.* (40) investigated the elastic-plastic fracture toughness via J-integral and crack tip opening displacement (CTOD) in structural steels using several fitting equations representing the resistance curve of material.

When a precracked specimen of a toughened polymer is under load, viscoelastic and inelastic micromechanisms such as crazing, cavitation, debonding, and shear yielding are expected to occur significantly around the crack tip region. These micromechanisms occur during the process of crack tip blunting (precrack) and during crack propagation. A portion of the storage energy is therefore consumed and a relatively large crack tip plastic zone is formed, which can be quantified by the corresponding hysteresis energy. The crack tends to propagate within the plastic zone and results in stable crack extension for rubber toughened polymer materials. In our recent studies of the fracture toughness of the elastomer modified polycarbonate (41, 42), HIPS (43, 44), ABS (45), PC/ABS blend (46–48), and PC/PBT blend (49–51), we proposed a new J-Integral method based on hysteresis properties of polymeric materials and the J_{Ic} values obtained were close to the E813-81 method but significantly lower than those from the E813-87 method. Experimentally this newly proposed J-Integral method is relatively simple, because the tedious measurement of crack growth length is not necessary. Whether this hysteresis approach can generally apply to all ductile and toughened polymeric materials, additional systems have to be tested. In this study, we will test the validity of this hysteresis energy method by comparing the J_{Ic} values of a PC/ABS blend by varying strain rate based on the E813-81, E813-87, and hysteresis methods.

J-INTEGRAL BY HYSTERESIS ENERGY METHOD

There are many practical cases in laboratory tests where it is necessary to evaluate a grossly nonlinear dissipative system. Such a situation was treated by Andrew and Fukahori (52, 53) using a generalized theory. However, this approach requires complicated and time-consuming experiments as well as some assumptions on the nature of the hysteresis behavior. According to Andrew's generalized fracture mechanics theory (52, 53), the fracture energy of a solid is given by:

$$\Im = \Im_o \Phi(\varepsilon_o, \dot{a}, T) \tag{1}$$

where $\Im$ is the total fracture energy of the system to cause a unit area of growth; $\Im_o$, the energy to rupture the unit area of inter-atomic bonds across the fracture plane (the "surface energy" of the body); and Φ, a loss function depending on the crack velocity ($\dot{a}$), the temperature (T), and applied strain (ε_o). The loss function

is derived as follows:

$$\Phi = K_1(\varepsilon_0) \Big/ \left[K_1(\varepsilon_0)^{-1/2} \left(\sum_{PU} \beta(x, y) \cdot g \cdot \delta_x \cdot \delta_y \right) \right] \quad (2)$$

where K_1 is a function of strain, x and y are the reduced cartesian coordinates of point P, g is a distribution function of the energy density, δ_x and δ_y are the volume element, $\beta(x, y)$ is the hysteresis ratio at point P, and the symbol PU denotes summation over points that unload as the crack propagates. The evaluation of the term $\Sigma_{PU}\beta(x, y)\cdot g\cdot\delta_x\cdot\delta_y$ of *Eq 2* requires an additional knowledge of the hysteresis ratio β from point to point in the stress field, and β will, in general, be a function of the local strain, strain rate, and temperature. Indeed, β will also, in general, depend on the amount of crack growth, Δa, since the functional energy loss at P will depend on the degree of relaxation permitted to occur there. However, for a steady-state tearing (constant crack speed), as observed in the work reported here, it is appropriate to use the hysteresis ratio for a full loading/unloading stress cycle at the appropriate strain rate. We have assumed that the β is a unique function of input energy density at a given strain rate.

Rubber-toughened polymeric materials exhibit significant internal energy dissipation of the crack tip region and the strain energy for crack propagation is the input energy minus the hysteresis (loss) energy as indicated in *Fig. 1*. This approach assumes that there is a region surrounding the crack tip with local energy dissipation. This arises from viscoelasticity, plasticity, and bond rupture and can be considered the characteristic of the fracture process. For polymers, the characteristic of this localized energy dissipation is considered to be independent of geometries.

The hysteresis ratio defined in this hysteresis energy method is not the same as the one developed by Andrew. It is the energy difference between the input and the recovery in the cyclic loading and unloading steps, which may include crack blunting and crack extension stages. The energy density change during crack growth can be presented by the following equation:

$$-dU/da = a \cdot W_o \left[\left(\sum_{PL} g(x, y) \cdot \delta_x \cdot \delta_y \right) - \left(\sum_{PU} G(\sigma_y, x, y) \cdot \delta_x \cdot \delta_y \right) \right] \quad (3)$$

where PL and PU indicate loading and unloading, respectively. W_o is the input energy density, and g and G are two functions of x, y, and σ_y, respectively. The quantity $-dU/da$ includes the energy available for forming crack surface and the energy consumed as plastic deformation of the cracked specimen. The input energy density W_o can be given by the area (A_o) under the loading curve up to a particular strain ε, and the recoverable energy density (W_r) is the area under the unloading covered (A_r). The hysteresis ratio [$HR(\%)$] is then defined by the following equation:

$$HR(\%) = (A_o - A_r)/A_o \quad (4)$$

and the hysteresis energy [HE (J)] is then given by:

$$HE(J) = HR(\%)U \quad (5)$$

where U is the input energy at different displacements.

For a cracked specimen, the material surrounding the crack tip can be divided into three parts: (1), the first plastic zone; (2), the second plastic zone; and (3), the elastic fracture surface. The specific energy balance equation for a cracked specimen can be expressed as the following:

$$(1/B)(dU/da - dU_e/da - dU_k/da) = (1/B) \cdot (dU_p^{PPZ}/da + dU_p^{SPZ}/da) + 2\gamma_s \quad (6)$$

and the energy dissipated of the system is given as:

$$dHE/Bda = (1/B)(dU_p^{PPZ}/da + dU_p^{SPZ}/da) + 2\gamma_s \quad (7)$$

where the U_k is the kinetic energy; U_e, the elastic energy, U_p^{PPZ}, the plastic energy for the primary plastic zone; U_p^{SPZ}, the plastic energy for the secondary plastic zone; and γ_s, the fracture surface energy. When a precracked specimen is under loading before the onset of crack extension (during blunting), a significant portion of the input energy is consumed and converted into a relatively larger crack tip plastic zone for the toughened polymers. These viscoelastic and inelastic energies may include many possible energy dissipated micromechanisms such as crazing, cavitation, debonding, and shear yielding, which can be related to the measured hysteresis energy. The hysteresis energy will increase gradually with the increase of load from the load vs. displacement curve. After crack extension, the strain energy release due to

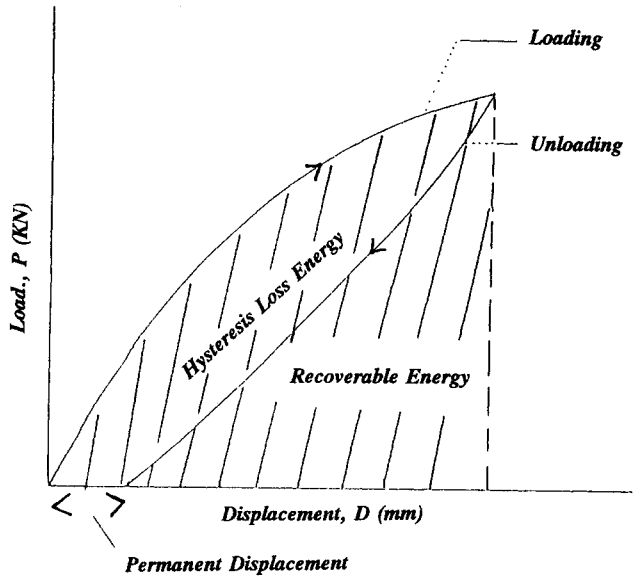

Fig. 1. ASTM SENB loading-unloading curve; the hatched area, A, is used to approximate the J-integral, i.e. J = 2A/(Bb).

crack growth will be added into the observed total hysteresis energy. The rate of the hysteresis energy increase due to this strain energy release is significantly higher than those above-mentioned precrack micromechanisms. Therefore, in a plot of hysteresis energy vs. deformation displacement of a notched specimen, a clear transition from crack blunting to crack extension can be identified. Such a phenomenon, a drastic increase of the hysteresis energy immediately after the onset of the crack extension, can be used to determine the critical fracture toughness (J_{Ic}) at the onset of crack extension. The data observed to support this viewpoint were presented in our previous articles (41–51).

METHODS

Injection molded PC/ABS specimens with dimensions of 20 × 90 × 10 mm, were prepared by an Arbury injection molding machine as *Fig. 2*. All specimens were notched with a fresh razor blade. All the notched specimens were annealed at 60°C for 2 h to release the residual stress prior to the standard three-point bend testing. The *J*-integral testing was carried out according to the multiple-specimen method outlined in ASTM E813 method at ambient conditions by varying the testing rate from 0.5 to 20 mm/min. The crack growth length was measured at the center of the fracture surface by freezing the deformed specimens in liquid nitrogen then propagating the crack through the specimen with a TMI pendulum impact tester. Hysteresis tests were carried out by loading at a constant rate to a pre-determined displacement then unloading at the same rate.

RESULTS AND DISCUSSION

J_{Ic} Determination by ASTM Standards and Modified Versions

The multiple-specimen technique is used to load the specimen to a controlled displacement and then is unloaded following the ASTM method. Detailed data for the specimens with B = 10mm at rate of 10 mm/min are summarized in *Table 1*. *Figure 3* is a plot of the acceptable J vs. Δa by linear regression line according to ASTM E813-81. This linear regression intersects with the blunting line to define the critical $J_{Ic\text{-}81}$ value.

Table 1. The Typical Data of the PC/ABS Blend at Rate = 10 mm/min.

D (mm)	*U* (*J*)	*J* (*KJ/m²*)	*HR* (%)	*HE* (*J*)	*Δa* (mm)
1.0	0.089	1.78	2.02	0.0017	0.032
1.2	0.193	3.86	4.66	0.0090	0.059
1.3	0.211	4.22	6.95	0.0147	0.075
1.4	0.230	4.60	7.68	0.0177	0.096
1.5	0.285	5.70	12.04	0.0343	0.153
1.6	0.321	6.42	14.82	0.0475	0.184
1.7	0.370	7.40	16.87	0.0624	0.247
1.8	0.435	8.72	19.86	0.0864	0.268
1.9	0.453	9.06	21.58	0.0978	0.321
2.0	0.527	10.54	24.26	0.1279	0.402
2.1	0.594	11.80	27.74	0.1648	0.560
2.3	0.674	13.48	31.31	0.2110	0.671
2.4	0.711	14.22	33.27	0.2265	0.683
2.6	0.754	15.08	37.68	0.2826	0.754
2.7	0.830	16.60	39.96	0.3322	0.789
2.8	0.896	17.92	42.73	0.3829	0.877
3.0	0.987	19.42	49.62	0.4897	1.071

D: Displacement (mm).
U: Input Energy (*J*).
J: *J*-Integral (KJ/m²).
HR: Hysteresis Ratio (%).
HE: Hysteresis Energy (*J*).
Δa: Crack Growth Length (mm).

The $J_{Ic\text{-}81}$ values obtained by E813-81 are generally independent of the crosshead speed varying from 0.5 to 20 mm/min. Another critical J_{Ic} value ($J_{o\text{-}81}$) was determined at the interception of the linear regression resistance curve with the *Y*-axis as recommended by Narisawa and Takemori (23), the obtained $J_{o\text{-}81}$ is slightly lower (~15 to 20%) than that from the E813-81 method due to the neglect of the crack blunting phenomenon of the crack tip. All these data from ASTM E813-81 and its modified methods at different rates are summarized in *Table 2*.

In ASTM E813-87 method, the values of the C_1 and C_2 of the power law line, $J = C_1(\Delta a)^{C2}$, are obtained from the plot of ln(J) vs. ln(Δa) within the exclusion lines between Δa = 0.15mm and Δa = 1.5mm and are summarized in *Table 2*. The J_{Ic} is then located at the intersection of the power law fit line and the 0.2mm offset line as shown in *Fig. 4* at a strain rate of 10 mm/min. The data obtained by the ASTM E813-87 method are also summarized in *Table 2*. The J_{Ic} values obtained from E813-87 method are ~60 to 80% higher

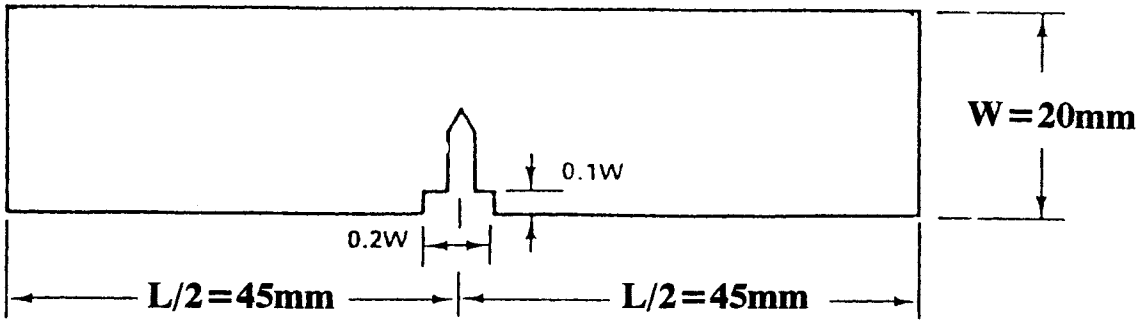

Fig. 2. Three-point-bending specimen geometry.

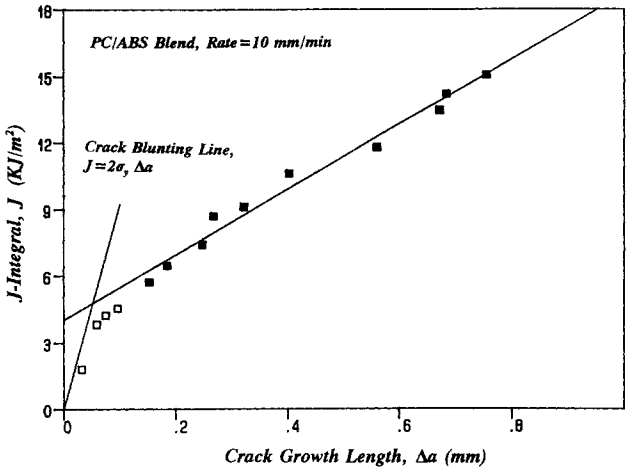

Fig. 3. Plot of J vs. crack growth length, Δa, according to ASTM E813-81 method at Rate = 10 mm/min.

than those from the corresponding E813-81 method. If the 0.2mm offset line specified in E813-87 is now reset at 0.1mm and the rest of the procedures are unchanged as shown in *Fig. 4*, the resultant J_{Ic} obtained now becomes comparable to that from E813-81 method (*Table 2*). Similar results were also obtained from our previous papers (49, 50). After all, the 0.2mm offset line suggested in the ASTM E813-87 standard is only an arbitrarily selected value to define the critical fracture toughness (J_{Ic}).

J_{Ic} Determination by the Hysteresis Method

The hysteresis ratio and energy of each specimen at different displacements are calculated by the *Eqs 4* and *5*, respectively. The results of the hysteresis ratio and hysteresis energy at different displacements are summarized in *Table 1*. The measured hysteresis energy is believed to be higher than the true hysteresis energy, because of the time-dependent nature of polymers. It is impossible to obtain the true hysteresis energy at the end point of loading. *Figure 5* combines the plots of the hysteresis energy and J vs. crosshead displacement at a rate of 10 mm/min. The crack initiation displacement (D_c) is located at the intersection between the blunting line and the power law propagation line. As soon as the D_c is located, the $J_{Ic\text{-}HE}$ is then determined from the plot of the J vs. displacement curve. Since the measurement of crack growth length is no longer necessary by this hysteresis energy method, it is relatively easier than the ASTM E813 methods. The $J_{Ic\text{-}HE}$ values obtained from the hysteresis energy method (*Table 3*) are ~10 to 20% higher than the $J_{Ic\text{-}81}$ values obtained from E813-81 method, but are ~50 to 70% lower than the $J_{Ic\text{-}87}$ values obtained from E813-87 method as shown in *Table 2*. However, the J_{Ic} values determined by the hysteresis energy method are comparable to those obtained from the modified ASTM E813-87 method by using an 0.1mm offset line. The use of an 0.1mm offset line to define the "best estimate" of crack initiation is discussed in detail in our previous papers (49, 50). The

Table 2. Critical J_{Ic} from ASTM E813 Methods.

ASTM E813-81 Method					
Rate (mm/min)	0.5	2	5	10	20
$J_{Ic\text{-}81}$, kJ/m²	4.85	4.65	4.86	4.80	4.06
$J_{Q\text{-}81}$, kJ/m²	4.05	3.89	4.10	4.03	3.45
ASTM E813-87 Method					
Rate (mm/min)	0.5	2	5	10	20
C_1	2059	1372	1744	1149	1129
C_2	0.674	0.625	0.653	0.654	0.612
$J_{Ic\text{-}87}$, KJ/m²	8.62	8.24	8.41	8.19	7.59
$J_{Q\text{-}87}$, KJ/m²	5.69	5.81	5.77	5.47	5.26

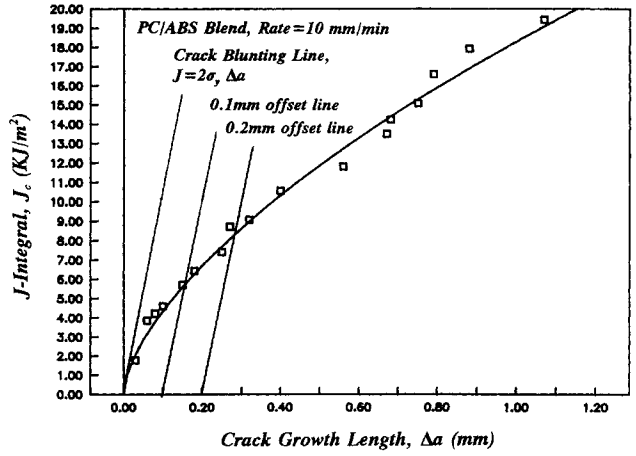

Fig. 4. Plot of J vs. crack growth length, Δa, according to ASTM E813-87 method at Rate = 10 mm/min.

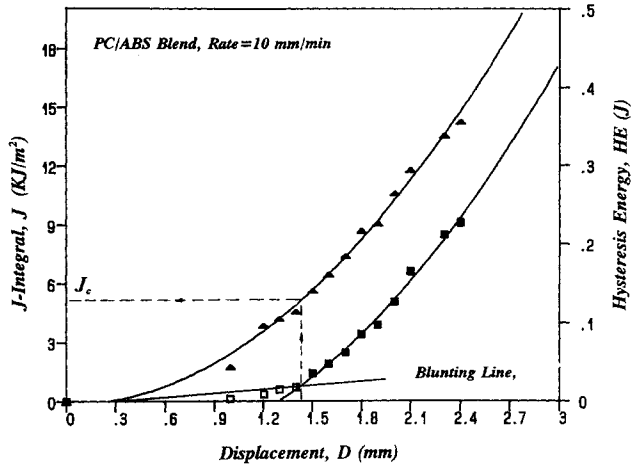

Fig. 5. The J_{Ic} value determination according to the hysteresis energy method at Rate = 10 mm/min.

plots of critical displacement obtained from the hysteresis energy and ratio vs. the strain rate is shown in *Fig. 6*, and the determined critical displacement from these two methods are very close and independent of the strain rate. The plot of the crack growth length vs. crosshead displacement at strain rate of 10 mm/min is shown in *Fig. 7*. The critical displacement is now located at the intersection between two linear regression lines. The critical displacements obtained lie between 1.45 ± 0.5 mm for rates varying from 0.5 to 20 mm/min. The critical displacements determined from

Table 3. Critical Displacement D_c and Critical J_{Ic} From the Hysteresis Energy Method at Rate = 2 mm/min.

Rate (mm/min)	0.5	2	5	10	20
$D_{c\text{-}HE}$, mm	1.48	1.44	1.43	1.46	1.48
$J_{Ic\text{-}HE}$, KJ/m^2	5.32	5.01	5.25	5.28	5.22
$D_{c\text{-}a}$, mm	1.43	1.39	1.43	1.47	1.40

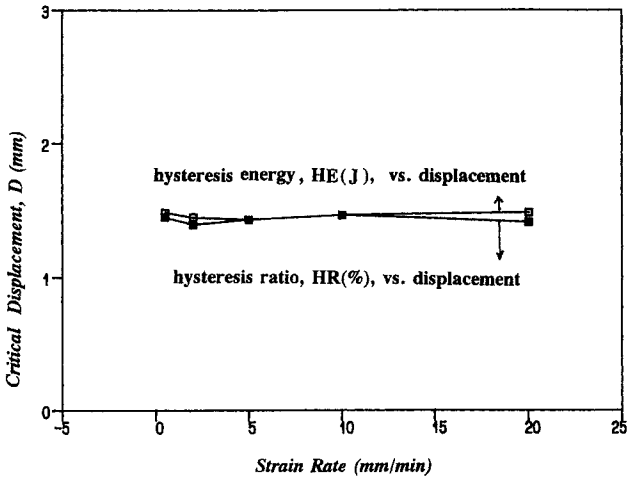

Fig. 6. Plots of the critical displacement, D_c, vs. the strain rate.

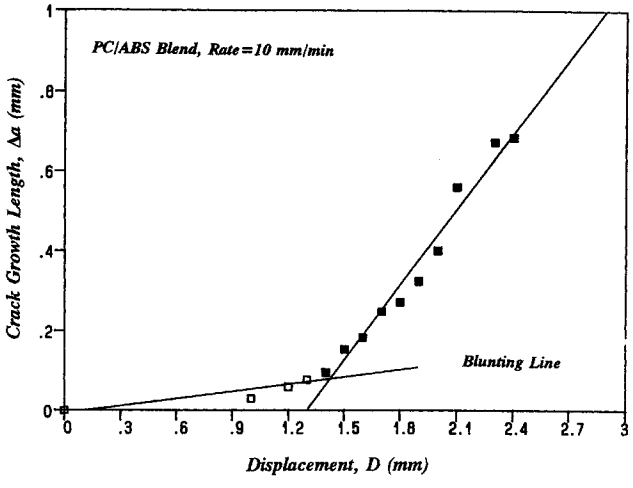

Fig. 7. Plot of the crack growth length, Δa, vs. displacement.

the plots of the hysteresis energy vs. displacement ($D_{c\text{-}HE}$) and crack growth length (Δa) vs. displacement ($D_{c\text{-}a}$), are also fairly close. That means the critical displacement from hysteresis energy methods is indeed the displacement due to the onset of crack extension. *Table 3* summarizes these two critical D_c and $J_{Ic\text{-}HE}$ values of PC/ABS blend at different rates by this hysteresis energy method. Finally, the critical *J*-integral values obtained from above various *J*-integral methods are presented in *Fig. 8*.

CONCLUSION

This hysteresis energy method is inherently adjustable for crack blunting. It thus avoids the controversy of blunting. It is also simple, without the requirement

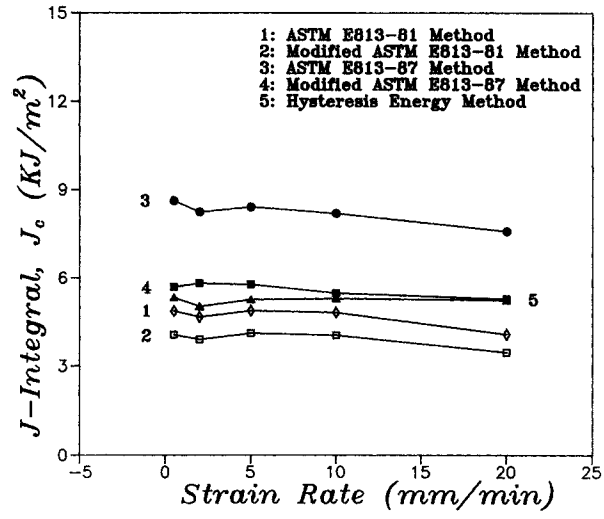

Fig. 8. Plots of the critical J_{Ic} value vs. the strain rate.

of the tedious crack growth length measurements. The J_{Ic} values obtained from the hysteresis energy method are ~10 to 20% higher than those obtained from the E813-81 method, but are ~50 to 70% lower than those from the E813-87 method, and are comparable to the modified E813-87 method. J_{Ic} values determined from the ASTM E813-81, E813-87, and hysteresis energy methods are largely independent of the test rate.

ACKNOWLEDGMENT

The authors are grateful to the National Science Council of Republic of China for the financial support.

REFERENCES

1. ASTM Standard E399-78, in *Annual Book of ASTM Standards*, part **10,** 54 (1978).
2. R. S. Rivlin and A. G. Thomas, *J. Polym. Sci.*, **10,** 291 (1953).
3. J. R. Rice, *J. Appl. Mech.*, **35,** 379 (1968).
4. J. R. Rice, in *Fracture, an Advance Treatise*, p. 192, H. Leibowitz, ed., Academic Press, New York (1979).
5. C. E. Turner, in *Post-Yield Fracture Mechanics*, p. 23, D. G. H. Latzko, ed., Applied Science Publishers Ltd., London (1979).
6. G. G. Chell, in *Developments in Fracture Mechanics*, p. 67, G. G. Chell, ed., Applied Science Publishers Ltd., London (1979).
7. J. D. Landes and J. A. Begley, in *Post-Yield Fracture Mechanics*, p. 211, D. G. H. Latzko, ed., Applied Science Publishers, Ltd., London (1979).
8. J. A. Begley and J. D. Landes, ASTM STP **514,** 1 (1972).
9. J. D. Landes and J. A. Begley, ASTM STP **560,** 170 (1974).
10. J. R. Rice, P. C. Paris, and J. G. Merkle, ASTM STP **536,** 231 (1973).
11. B. S. Westerlind, L. A. Carlsson, and Y. M. Andersson, *J. Mater. Sci.*, **26,** 2630 (1991).
12. ASTM Standard E813-81, in *Annual Book of ASTM Standards*, Part **10,** 822 (1982).
13. ASTM Standard E813-87, in *Annual Book of ASTM Standards*, part **10,** 968 (1987).
14. M. K. V. Chan and J. G. Williams, *Polym. Eng. Sci.*, **21,** 1019 (1981).
15. M. K. V. Chan and J. G. Williams, *Int. J. Fract.*, **19,** 145 (1983).

16. S. Hashemi and J. G. Williams, *Polym. Eng. Sci.*, **26,** 760 (1986).
17. S. Hashemi and J. G. Williams, *Polymer*, **27,** 85 (1986).
18. D. D. Huang and J. G. Williams, *J. Mater. Sci.*, **22,** 2503 (1987).
19. P. K. So and L. J. Broutman, *Polym. Eng. Sci.*, **26,** 1173 (1986).
20. E. J. Moskala and M. R. Tant, *Polym. Mater. Sci. Eng.*, **63,** 63 (1990).
21. C. M. Rimnac, T. M. Wright, and R. W. Klein, *Polym. Eng. Sci.*, **28,** 1586 (1988).
22. I. Narisawa, *Polym. Eng. Sci.*, **27,** 41 (1987).
23. I. Narisawa and M. T. Takemori, *Polym. Eng. Sci.*, **29,** 671 (1989).
24. D. D. Huang and J. G. Williams, *Polym. Eng. Sci.*, **30,** 1341 (1990).
25. D. D. Huang, *Polym. Mater. Sci. Eng.*, **63,** 578 (1990).
26. D. S. Parker, H. J. Sue, J. Huang, and A. F. Yee, *Polymer*, **31,** 2267 (1990).
27. A. Chudnovsky and A. Moet, *J. Mater. Sci.*, **20,** 630 (1985).
28. A. Chudnovsky and A. Moet, *Elast. Plast.*, **18,** 50 (1986).
29. N. Haddaoui, A. Chudnovsky, and A. Moet, *Polymer*, **27,** 1337 (1986).
30. A. Chudnovsky, A. Moet, R. J. Bankert, and M. T. Takemori, *J. Appl. Phys.*, **54,** 5562 (1983).
31. Y. W. Mai and B. Cotterell, *J. Mater. Sci.*, **15,** 2296 (1980).
32. Y. W. Mai and B. Cotterell, *Eng. Fract. Mech.*, **21,** 123 (1985).
33. Y. W. Mai, B. Cotterell, R. Horlyck, and G. Vigna, *Polym. Eng. Sci.*, **27,** 804 (1987).
34. J. Wu, Y. W. Mai, and B. Cotterell, *J. Mater. Sci.*, **28,** 3373 (1993).
35. T. Yuhara and M. T. Kortschot, *J. Mater. Sci.*, **28,** 3571 (1993).
36. J. A. Joyce and E. M. Hackett, ASTM STP **905,** 741 (1986).
37. T. Vu-Khanh, *Polymer*, **29,** 979 (1988).
38. B. A. Crouch and D. D. Huang, *J. Mater. Sci.*, **29,** 861 (1994).
39. Z. Zhou, J. D. Landes, and D. D. Huang, *Polym. Eng. Sci.*, **34,** 128 (1994).
40. J. F. Saze, J. Chao, J. Duran, and J. M. Amo, *J. Mater. Sci.*, **28,** 5340 (1993).
41. C. B. Lee and F. C. Chang, *Polym. Eng. Sci.*, **32,** 792 (1992).
42. C. B. Lee, M. L. Lu, and F. C. Chang, *J. Chinese Inst. Chem. Eng.*, **23,** 305 (1992).
43. C. B. Lee, M. L. Lu, and F. C. Chang, *J. Appl. Polym. Sci.*, **47,** 1867 (1993).
44. C. B. Lee, M. L. Lu, and F. C. Chang, *Polym. Mater. Sci. Eng.*, **64,** 510 (1992).
45. M. L. Lu, C. B. Lee, and F. C. Chang, *Polym. Eng. Sci.*, **35,** 1433 (1995).
46. M. L. Lu, C. B. Lee, and F. C. Chang, *J. Appl. Polym. Sci.*, to appear.
47. M. L. Lu and F. C. Chang, *Polymer*, **36,** 2541 (1995).
48. M. L. Lu and F. C. Chang, *Polymer*, to appear.
49. M. L. Lu and F. C. Chang, *J. Appl. Polym. Sci.*, **56,** 1065 (1995).
50. M. L. Lu and F. C. Chang, *Polymer*, **36,** 4639 (1995).
51. M. L. Lu and F. C. Chang, *J. Polym. Res.*, **2,** 13 (1995).
52. E. H. Andrews, *J. Mater. Sci.*, **9,** 887 (1974).
53. E. H. Andrews and Y. Fukahori, *J. Mater. Sci.*, **12,** 1307 (1977).